

Conceptual Design of a Geostationary Radar for Hurricane Studies

Eastwood Im^{a*}, Eric A. Smith^b, Stephen L. Durden^a, Simone Tanelli^a, John Huang^a, Yahya Rahmat-Samii^c, Michael Lou^a

^a Jet Propulsion Laboratory, California Institute of Technology, Pasadena, CA 91109, USA

^b NASA Goddard Space Flight Center, Greenbelt, MD 20771, USA

^c University of California, Los Angeles, CA 90095, USA

Abstract – A novel 35-GHz Doppler radar instrument concept and the associated critical technologies are being developed for detailed monitoring of hurricanes and severe storms from a geostationary orbit. This instrument is designed to make quantitative rainfall rate profiling measurements at 13-km horizontal resolution and 300-m vertical resolution, and the radial Doppler velocity at 0.3 m/s precision, of the 3-D hurricane structure once per hour throughout its life cycle.

Keywords: Hurricane, precipitation, radar, geostationary

I. INTRODUCTION

Existing Geostationary Operational Environmental Satellites (GOES) have proven to be valuable in cloud meteorology, water vapor and surface temperature retrieval, and weather synopsis. However, the lack of cloud penetrating ability does not permit current GOES instruments to directly measure rainfall associated with hurricanes and severe storms.

Ground-based Doppler radars have long been used for monitoring severe precipitating storms. Unfortunately, they cannot observe hurricanes at their genesis or at the developing stage (i.e., the “out-of-sea” phase). Recently, the Precipitation Radar (PR) (Kozu et al. 2001) aboard the Tropical Rainfall Measuring Mission (TRMM) satellite has demonstrated an unprecedented capacity to cat-scan precipitating storms, and to enable improved understanding of hurricane structure. Nonetheless, due to the relatively long return cycle (less than once per day) the value of PR data has only been limited to understanding of hurricane’s climatological properties.

Radar remote sensing of the atmosphere and severe storms from geostationary orbit is highly desirable owing to the radar’s unique ability to simultaneously provide vertical rainfall profiles, large spatial coverage, and frequent observations. With the rapid advances in radar technology, the feasibility of developing such an instrument has greatly improved. Under NASA’s Earth Science Technology Program, a novel instrument concept and the associated antenna technologies are currently being developed for a 35-GHz Doppler radar for detailed monitoring of hurricanes, cyclones, and severe storms from a geostationary orbit. Since this radar approach is analogous to putting a NEXRAD system in orbit, it is being referred to as “NEXRAD in Space (NIS)”.

The advantage of a space radar’s ability to penetrate precipitating clouds relative to standard GOES cloud imagery is illustrated in Fig. 1. This figure emphasizes how TRMM PR information can be used quantitatively to gauge the intensity of a hurricane, its vertical rain rate structure, and its water carrying capacity. It is also evident that the complete and frequent hurricane coverages by a geo-profiling radar such as NIS will enable hurricane rain and cloud processes to be monitored over much of their life cycle, thus providing the temporal information needed for creating advanced flood and hazard warning systems,

improving numerical model prediction of hurricane tracks and landfalls, and understanding more about the hurricane diurnal cycle. Furthermore, the cloud penetration ability of the radar will allow quantitative measurements of the vertical structures of both non-precipitating and precipitating clouds. This is of particular importance in addressing how cloud-radiation feedbacks and atmospheric hydrological cycle responds to external influences (such as deep ocean circulation induced warmings and coolings). The NIS measurements, when used together with existing GOES measurements, can deduce vertical and horizontal cloud structure for the study and monitoring of solar and infrared radiative transfer in heterogeneous cloudy atmospheres, the essential ingredients for accurate diagnosis of the Earth’s radiation budget and the atmosphere’s radiative heating-cooling behavior.

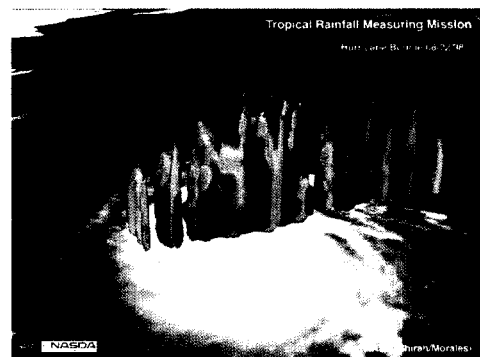


Fig. 1: TRMM PR acquired vertical rain profiles of Hurricane Bonnie overlaid on the corresponding GOES image.

II. NOVEL RADAR OBSERVATIONAL CONCEPT

NIS is designed to operate in the geostationary orbit at an altitude of 36,000 km. From the trade study between spatial resolution and rain penetration/profiling, we have selected 35 GHz as the radar frequency. A deployable, 30-m, spherical antenna reflector will be used together with two antenna feeds, one for signal transmission and the other for echo reception, to form the overall antenna subsystem. Both the reflector and the spacecraft will remain stationary as the antenna feeds perform spiral scans up to 4° from boresight to cover a 5300-km circular disk on the Earth surface. This coverage is equivalent to 48° (±24°) in both longitude and latitude. If necessary, small spacecraft maneuver can be used to extend the latitudinal coverage. This scan approach allows continuous and smooth transition between adjacent radar footprints. One complete disk scan will require 200 spirals. The NIS surface coverage is graphically illustrated in Fig. 2, and the average time required for each spiral is given in Fig. 3. The corresponding horizontal resolution ranges from 12 km at nadir to 14 km at 4° scan.

The dual-feed approach is used to compensate for the long range distance. The angular spacing between the transmit and receive

* Corresponding author. E-mail: eastwood.im@jpl.nasa.gov

feeds is designed to be 0.45° such that the rain echoes can be captured 0.25 seconds after pulse transmission. This approach also enables a two-fold increase in the number of radar echo samples obtained, which translates into a factor of 1.4 reduction in measurement noise. As the feeds scan through the spiral, the radar will continuously transmit radar pulses at a rate of 3.5 KHz. This selected rate will allow a vertical observation window of 25 km and will accommodate the changes in range distance throughout the spiral scans. The spiral scan rate as shown in Fig. 3 is designed to obtain one full disk coverage within 60 minutes and to allow a constant dwell time on each radar resolution cell.

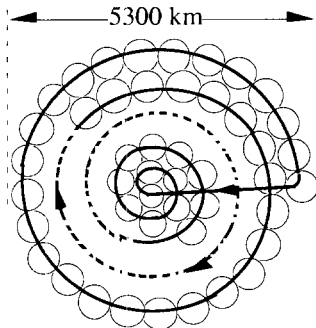


Fig. 2: Illustration of surface coverage by the spiral scan pattern.

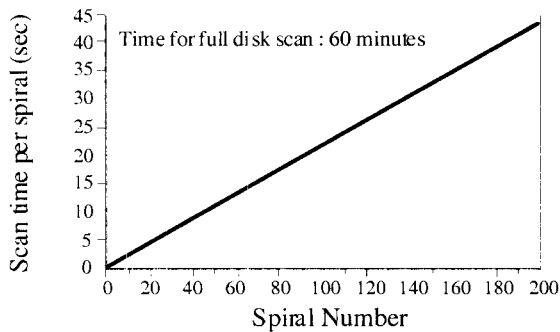


Fig. 3: Time per spiral (from inner-most to outer-most spiral).

III. REVOLUTIONARY ANTENNA CONCEPT

The NIS antenna requirements include an antenna gain of 77 dB, a beamwidth of 0.02° , a sidelobe level of better than -30 dB, and a scan of up to 4° off its axis. This angular scan translates into a scan of ± 200 beamwidths. The first potential antenna candidate is an electronically scanned array antenna. However, such a large array at 35 GHz would require over 6 million array elements. This is indeed a formidable and very expensive task. A second candidate is a parabolic reflector antenna. However, such antenna suffers from severe limitation at large beam scans. A focal plane array can potentially compensate for this performance degradation. Such implementation, however, necessitates the use of an active array with adaptively varying excitation coefficients for different look angles. Such an implementation could also become an expensive proposition. The third candidate is a mechanically rotating antenna. For such a large antenna, the torque created by rotating the entire reflector will be very large. The fourth candidate is a spirally-rotating spacecraft with a fixed-mounted antenna. This option, can be very complicated and requires extensive interface between the radar and the spacecraft. For NIS, we focus on a novel spherical reflector antenna design (Rahmat-Samii, 1989) which is capable of

scanning its beams to any desired direction without compromise on the radiation performance. Any spherical aberration-induced degradation will be overcome by using a small planar array in the focal plane. Such a focal array can achieve any desired beam direction; more importantly, there is no need to reconfigure the array excitation coefficients for new beam direction.

Spherical reflector antennas produce almost identical beams when their feeds are rotated with respect to the focal point. The major drawback is the excessive gain loss due to the presence of an extended focal region. Since the objective is to cover a $\pm 4^\circ$ angular range, we will use an oversized reflector antenna at 30m diameter to cover the desired angular range by utilizing sub-apertures for various beam look angles. This antenna configuration is graphical illustrated in Fig. 4. Our initial parametric study showed that the utilization of a 271-element, rotating, fixed feed array with complex excitation coefficients would substantially improve the performance of the spherical reflector antenna. The size of the feed array is ~ 20 cm in diameter. The corresponding antenna radiation patterns at 4° scan are shown in Fig. 5. Note that an antenna gain of ~ 80 dB with sidelobe levels below 30 dB are obtained.

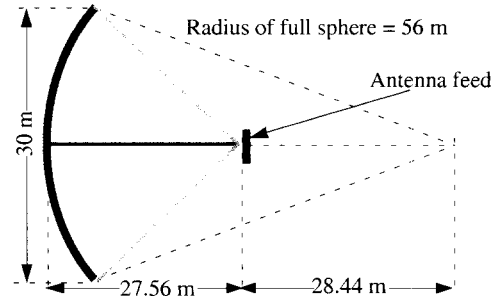


Fig. 4: Geometry of the NIS spherical reflector antenna.

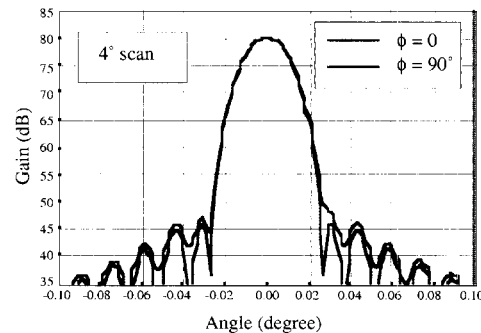


Fig. 5: NIS antenna patterns at 4° off-axis.

The two feed arrays will be mechanically moved on a spiral track. One mechanism which achieves the desired motion is a rotating arm which carries a trolley containing the two feeds. The trolley travels along the axis of the arm on precision wheels preloaded against precision rails.

IV. DEPLOYABLE ANTENNA MECHANICAL DESIGN

From mass and size considerations, three mechanical reflector concepts can potentially be adapted for the NIS antenna application. The first concept, shown in Fig. 6(a), employs the emerging space inflatable technology. When deployed, the reflector assumes a lenticular shape formed by two spherical

thin-film membrane halves. One of the membrane halves is coated and functions as the reflective surface. The other membrane half is a transparent canopy, with the sole function of holding the extremely low (about 10-4 psi) inflation pressure. A circular torus and three struts, all are made of membrane materials and are inflation deployable and space rigidizable, provide structural support for the reflector. Ultra-flex solar arrays that have membrane substrates can be mounted on the surface of the torus. Development of flexible solar arrays with higher efficiency is currently being carried out mainly under the sponsorship of DoD. Based on ground measurements of a 14-m off-axis parabolic reflector developed for the Inflatable Antenna Experiment (IAE) launched with the shuttle mission in 1996, the best as-manufactured surface accuracy for an on-axis spherical inflatable reflector is expected to be in the range of 0.5 to 1 mm RMS. To further improve the surface accuracy, adaptive shape control can be used for on-orbit configuration adjustments.

The second design concept in Fig. 6(b), uses the AstroMesh reflector approach. Structurally, this reflector consists of a cable-actuated synchronized parallelogram mechanism (that deploys the reflector) and a pair of ring-stiffened, tension-tied geodesic domes. The reflective mesh is stretched over the back of one of the domes. Based on the measured surface error of less than 0.36 mm RMS on the Astro's 6-m flight model, and the considerations on several potential design improvements, including denser geodesic net structures, CTE tailoring, thinner webs, and refined materials conditioning, a 30-m AstroMesh reflector should meet the 0.75-mm RMS performance goal. Since sunrays can pass the mesh, traditional solid solar array panels attached to the spacecraft bus can be used for this option.

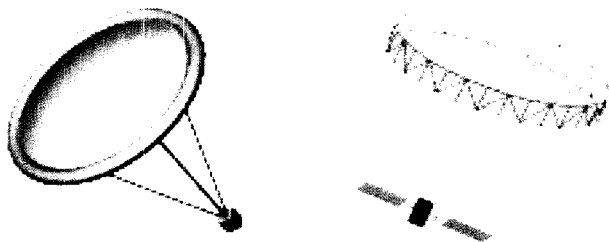


Fig. 6: (a) Inflatable reflector approach; (b) AstroMesh approach.

The third concept option is a hybrid of the first two concepts. It uses the mesh to deploy a reflective thin-film (less than 1 mil) antenna aperture for improved RF performance. In this case, the mesh can be made of thin lightweight wires and the grids of the mesh can be relatively coarse. With a slightly increased reflector diameter, an annular ring of ultra-flex membrane solar arrays can be incorporated around the antenna aperture to eliminate the need for traditional solid solar panels.

V. PULSE COMPRESSION TECHNIQUE

Since raindrops are weak scatterers, rain mapping demands substantially higher peak power. Pulse compression approach can be used to remediate this problem. This approach is simple: long, frequency-modulated pulses containing substantially more energy are transmitted and the radar echoes are compressed in range such that most of the echo energy is re-focused into the range bins which contain the rain returns. In the NIS design, 100- μ sec frequency-modulated pulses and 0.6-MHz bandwidth will be used to increase the effective detection sensitivity by 18

dB, while maintaining a respectable 300-m vertical resolution. The designed transmitter peak power is at a moderate 100-W level. The key challenge on pulse compression is the signal contamination by ground clutters through the range sidelobes. At 35 GHz, the required sidelobe suppression level is about -52 dB. However, several airborne rain radar systems, such as the NASA/JPL's 14-GHz Airborne Rain Mapping Radar (Durden et al., 1994) and 14/35-GHz Second-Generation Precipitation Radar (Im et al., 2000), have consistently demonstrated a 60-dB range sidelobe suppression capability.

VI. RADAR ELECTRONICS CONCEPT

NIS RF electronics consists of an Arbitrary Waveform Generator (AWG) to synthesize the chirp waveform, an upconverter and a receiver. Using AWG instead of the traditional numerically controlled oscillator has the benefits of implementing amplitude weighting and predistortion of the linearly frequency-modulated pulses in order to compensate for non-ideal characteristics of the system. The chirp waveform is generated at an IF frequency and upconverted to 35 GHz using a two-stage mixing process. The LO frequencies are provided by phase-locked oscillators and dielectric resonator oscillators, which are all locked to a reference oscillator for coherent up and downconversion. Distributed signal amplification approach is used in which a 0.5-watt solid-state power amplifier (SSPA) will be placed between each radiating element and the waveguide power divider. A total of 271 0.5-watt amplifiers are therefore needed. One-watt 35-GHz SSPAs are being developed jointly by NASA's Earth and Space Science programs (Sadowy et al., 2001). Distributed 35-GHz receiver modules are used in the receive array feed to amplify and downconvert the radar echoes to IF. The distributed IF signals are then combined and downconverted to offset video.

The digital electronics subsystem includes control and timing unit, analog-to-digital converter, multiplexer, data processor, and data formatter. The control and timing unit decodes all radar mode commands and generates the required timing signals. It also controls the timing of the antenna beam scan. The 14-bit ADCs, with dynamic range greater than 70 dB, digitize the linearly detected video signals. The digitized data is multiplexed and sent to the onboard data processor. The data processor performs on-board processing of the data acquired by NIS. The processed data are formatted and sent to the tape recorder for storage. One full disk scan of radar image will be downlinked to the ground station every hour.

VII. ON-BOARD DATA PROCESSING

The objectives of on-board data processing are to process the acquired backscattered measurements in near real-time fashion and to reduce the downlink data rate such that the 3-dimensional rainfall imagery can be generated once every hour. The on-board data processing includes pulse compression, pulse averaging, and pulse pair Doppler processing. Pulse compression requires that the received signal be correlated with a replica of the transmitted signal. Achieving low range sidelobes requires that the pulse compression processing be done digitally. When pulse compression is completed, the complex voltage is averaged to estimate power and Doppler. After on-board data processing, the output data rate is reduced to ~160 kbits/sec. For the NIS application we will adapt the programmable digital signal processor which has been successfully prototyped through the PR-2 technology development task (Berkun et al., 2002), within NASA's Earth Science Instrument Incubator Program. This real-

time processor is a COTS VME board made by Annapolis Microsystems. The board contains three Xilinx Vertex field programmable gate arrays (FPGAs). This processor prototype performs pulse compression, averaging, and Doppler for four receiver channels at the rate of 20 billion multiplications and 20 billion additions per second, a throughput equivalent to about 20 general-purpose processors working in parallel.

VIII. NIS Radar Parameters and Estimated Performance

The key NIS instrument and performance parameters are summarized in Table 1. Note that by an averaging of 120 pulses, the NIS detection sensitivity is improved to ~ 5 dBZ. The rain signal-to-noise ratios (SNRs) in Fig. 7 show that NIS can indeed achieve significant rain penetration. For example, NIS can measure ~ 35 mm/hr rain down to 2.5 km from the cloud top. At higher rain rates, the attenuation become significant and NIS's penetration ability reduces.

Radar System Parameters			
Frequency	35 GHz	Bandwidth	0.58 MHz
Antenna diameter	30 m	Pulsewidth	100 μ sec
Ant. effective aperture	28 m	PRF	3.5 KHz
Ant. 3-dB beamwidth	0.019°	Power duty cycle	35%
Antenna gain	77.2 dBi	Transmit path losses	2 dB
Antenna sidelobe	-30 dB	Receive path losses	2 dB
Max. spiral scan angle	4°	Sys. noise temp.	910 K
Time for a full scan	60 mins.	Dynamic range	70 dB
Peak power	100 W	Downlink data rate	155 kbps
Performance Parameters			
Disk coverage diameter	5300 km	Doppler Precision	0.3 m/s
Vertical resolution	300 m	Pulse samples	120
Horiz. Resolution (nadir)	12 km	Min. Zeq (1 pulse)	15.4 dBZ
Horiz. Resolution (4°)	14 km	Min. Zeq (after ave.)	5.0 dBZ

Table 1: NIS radar parameters.

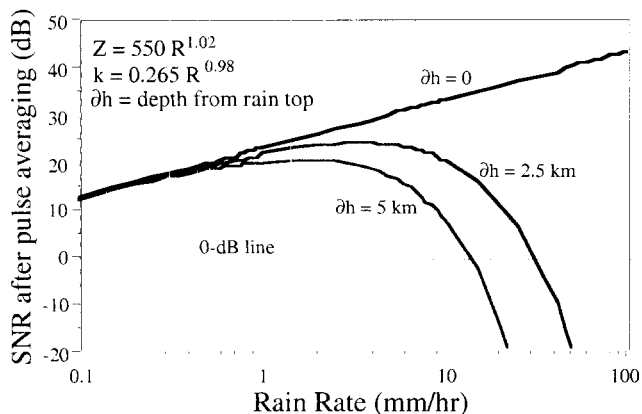


Fig. 7: SNRs for the NIS rain measurements.

Like all downward pointing precipitation radars, the NIS return signals from light rain can be contaminated by the simultaneous surface returns when the antenna is scanned away from nadir. However, since the rain rates associated with hurricanes and the 35-GHz rain attenuation are high, the surface clutter contamination is much less an issue than one might expect. To articulate this point, we computed the ratios of the rain signal to the combined noise and clutter (SNCR) at different rain rates. An example at 5 mm/hr rain over the ocean is shown in Fig. 8. At or near nadir the SNCR is dominated by thermal noise. Between $\sim 5^\circ$

and 15° incidence angles and at lower altitudes, the surface clutter becomes dominant. At larger incidence angles the clutter effect is reduced due to increased attenuation and weaker surface backscattering. The results thus show that at 5 mm/hr rain NIS can indeed penetrate down to lower than 2 km altitude at most incidence angles of interest. At larger rain rates the detectability is determined by attenuation and thermal noise, not clutter.

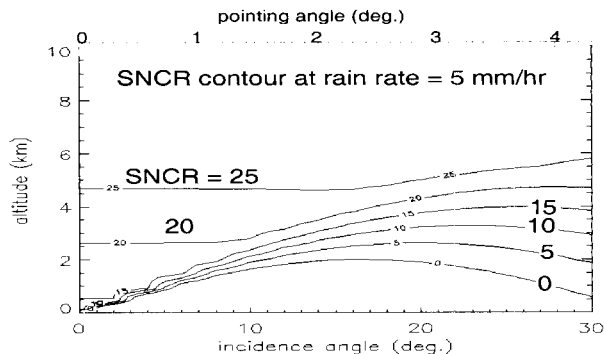


Fig. 8: SNCRs for the NIS at 5 mm/hr rain.

IX. SUMMARY

NASA's Earth Science Program is currently developing the technology for the NEXRAD In Space (NIS) instrument concept - a 35-GHz, spiral scanning Doppler radar for detailed monitoring of hurricanes, cyclones, and severe storms from a geostationary orbit. This instrument is designed to be capable of producing rainfall rate at 13-km horizontal resolution and 300-m vertical resolution, and the line-of-sight Doppler velocity at 0.3 m/s precision, of the 3-D hurricane structure once per hour throughout its life cycle.

ACKNOWLEDGMENTS

The research described in this paper was performed by the Jet Propulsion Laboratory, California Institute of Technology, under contract with the National Aeronautics and Space Administration.

REFERENCES

- T. Kozu et al., "Development of precipitation radar onboard the Tropical Rainfall Measuring Mission (TRMM) satellite" *IEEE Trans. Geosci. Remote. Sensing*, vol. 39, pp. 102-116, 2001.
- Y. Rahmat-Samii, "Improved reflector antenna performance using optimized feed arrays" *Proc. of 1989 URSI Intl. Sympos. on Electromagnetic Theory*, pp. 559-561, Stockholm, Sweden, August 14-17, 1989.
- S. L. Durden et al., "ARMAR: An airborne rain-mapping radar" *J. Atmos. Oceanic Technol.*, vol. 11, pp. 727-737, 1994.
- E. Im et al., "System Concept for next-generation spaceborne precipitation radars" *Proc. IEEE Aerosp. Sympos.*, pp. 151-158, Big Sky, Montana, 2000.
- G. Sadowy et al., "Technologies for the next generation of spaceborne precipitation radars" *Proc. IEEE Aerosp. Sympos.*, pp. 1811-1823, Big Sky, Montana, 2001.
- A. C. Berkun, M.A. Fischman, and E. Im, "An Advanced on-board processor and adaptive scanning controller for the next-generation precipitation radar" *Proc. Earth Sci. Technol. Conf.*, Pasadena, California, 2002.